



## Role of Some Benzohydrazide Derivatives as Corrosion Inhibitors for Carbon Steel in HCl Solution

A.S. Fouda<sup>\*1</sup>, M. T. Mohamed<sup>2</sup>, and M.R. Soltan<sup>1</sup>

<sup>1</sup>Department of Chemistry, Faculty of Science, El-Mansoura University, El-Mansoura-35516, Egypt

<sup>2</sup>Department of Chemistry, Faculty of Science (Damietta), El-Mansoura University, Damietta, Egypt

### ABSTRACT :

Corrosion inhibition of carbon steel in 2 M HCl by some benzohydrazide derivatives (I-III) was studied using weight loss, potentiodynamic polarization, and electrochemical impedance spectroscopy (EIS) techniques at 30°C. Polarization studies showed that all the investigated compounds are of mixed type inhibitors. Temperature studies revealed a decrease in efficiency with rise in temperature and corrosion activation energies increased in the presence of the hydrazide derivatives, probably implying that physical adsorption of cationic species may be responsible for the observed inhibition behavior. Electrochemical impedance studies showed that the presence of benzohydrazide derivatives decreases the double layer capacitance and increases the charge transfer resistance. The adsorption of these compounds on carbon steel surface was found to obey Temkin's adsorption isotherm. Synergistic effects increased the inhibition efficiency in the presence of halide additives namely KI and KBr. An inhibition mechanism was proposed in terms of strongly adsorption of inhibitor molecules on carbon steel surface.

**Keywords:** Metals, Corrosion, Inhibition, Polarization, EIS

Received May 29, 2013 : Accepted June 24, 2013

### 1. Introduction

Acid solutions are widely used in a variety of industrial processes such as acid pickling, industrial acid cleaning, acid decaling and oil well acidification,<sup>1)</sup> which generally lead to serious metallic corrosion. Because of the general aggressivity of acid solutions, inhibitors are commonly used to reduce the corrosive attack on metallic materials. Most of the well-known acid inhibitors are organic compounds containing nitrogen, oxygen, phosphorous, sulfur and aromatic ring or triple bonds. It was reported before that the inhibition efficiency decreases in the order: O < N < S < P.<sup>2-5)</sup> In general, organic compounds are effective inhibitors of aqueous corrosion of many metals and

alloys. The use of chemical inhibitors to decrease the rate of corrosion processes of carbon steels is quite varied.<sup>6-10)</sup> A variety of organic compounds containing heteroatoms such as O, N, S and multiple bonds in their molecule are of particular interest as they give better inhibition efficiency than those containing N or S alone.<sup>11-12)</sup> Sulfur and/or nitrogen containing heterocyclic compounds with various substituents are considered to be effective corrosion inhibitors. Benzohydrazide derivatives offer special affinity to inhibit corrosion of metals in acid solutions.<sup>13-16)</sup> Azoles have been intensively investigated as effective steel corrosion.<sup>17-21)</sup>

The increase in inhibition efficiency of organic compounds in the presence of some ions has been reported by some authors and was ascribed to the synergistic effect.<sup>22-24)</sup> Synergism has become a very important effect in corrosion inhibition processes and serves as

\*Corresponding author. Tel.: +2 050 2365730

E-mail address: asfouda@mans.edu.eg

the basis for most modern inhibitor formulations. Kalman *et al.*<sup>25)</sup> reported the synergistic increase in inhibition efficiency of hydroxyl-ethane-1, 1-diphosphonic acid in the presence of divalent cations such as  $Zn^{2+}$ . Similar effects have been observed in the presence of some anions, particularly halide ions. Gomma<sup>22)</sup> studied the effect of halide ions on the inhibition efficiency of pyrazole derivatives and observed that the synergistic effect increased in the order  $Cl^- < Br^- < I^-$ . Oguzie<sup>24)</sup> reported similar observation for the influence of halide ions on the inhibitive action of some organic dyes. Zhang *et al.*<sup>26)</sup> reported the synergistic effect of iodide ions on the efficiency of benzotriazole. Fouda *et al.*<sup>27)</sup> also reported the synergistic effect of some anions on the inhibition efficiency of p-thiazolidinone derivatives.

The present study aimed to investigate the inhibiting effect of some new benzohydrazide derivatives on carbon steel corrosion in 2 M HCl solution using chemical and electrochemical techniques. The effect of temperature as well as the synergistic effect of halide additives on the inhibition efficiency has also been studied. Kinetic and activation parameters that govern metal corrosion have been evaluated.

## 2. Experimental Details

### 2.1. Material

Prior to all measurements, the sheet samples (0.200% C, 0.350% Mn, 0.024% P, 0.003% Si and Fe balance) were abraded with a series of emery papers from 400 to 1200 grades. The specimens were washed thoroughly with bidistilled water, degreased with acetone and air dried. The solutions were prepared by dilution of analytical grade 37% HCl with bidistilled water in the absence and presence of inhibitors in the concentration range from  $3 \times 10^{-5}$  to  $15 \times 10^{-5}$  M. All the experiments were performed at  $30 \pm 1^\circ C$ .

### 2.2. Inhibitors

The inhibitors (benzohydrazide derivatives) were synthesized by following the literature procedure<sup>12)</sup> by reacting equimolar mixture of the respective aldehyde and hydrazide in 100 ml boiling ethanol. The mixture was refluxed on water bath for 2-6 hrs and the solution was evaporated to about its half volume, left to cool where crystals were separated out. These were filtered off, recrystallized from ethanol and finally dried in vacuum desiccator over anhydrous  $CaCl_2$ . The benzohydrazide derivatives structures were confirmed

by elemental analysis, IR and NMR spectroscopy and are shown in Table 1.

### 2.3. Weight loss measurement

The weight loss experiments were performed at 30, 35, 40, 45, 50 and  $55 \pm 1^\circ C$  with different concentrations of inhibitor. The optimized immersion time is 3 h. The results of weight loss experiments are the mean of three runs, each with a fresh specimen (2 cm  $\times$  2 cm  $\times$  0.2 cm) and 100 mL of fresh acid solution. The inhibition efficiency (% IE) and surface coverage ( $\theta$ ) were calculated using the following equation:

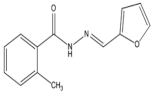
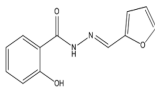
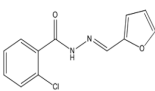
$$\% IE = \theta \times 100 = [1 - (\Delta W_{inh} / \Delta W_{free})] \times 100 \quad (1)$$

where  $\Delta W_{inh}$  and  $\Delta W_{free}$  are the weight losses per unit area in presence and absence of the inhibitor, respectively.

### 2.4. Potentiodynamic polarization measurements

Electrochemical polarization experiments were carried out in a traditional three-electrode glass cell with a capacity of 250 ml. A platinum sheet and a saturated calomel electrode (SCE) were used as a counter and reference electrodes, respectively. The working electrode was in the form of a square cut from carbon steel with surface area 1 cm  $\times$  1 cm. Before each experiment, the working electrode was polished mechanically, washed with acetone, rinsed several times with bidistilled water and dried. All tests have been performed with freshly polished electrode in deaerated test solution. A time interval of about 30 minutes was

**Table 1.** The names, structures, molecular weights and molecular formulae of the investigated benzohydrazide derivatives

Name	Structure	Molecular weight & Molecular formula
(I) (E)-N'-((furan-2-yl)methylene)-2-methyl benzohydrazide		$C_{13}H_{12}N_2O_2$ 228.3
(II) (E)-N'-((furan-2-yl)methylene)-2-hydroxy benzohydrazide		$C_{12}H_{10}N_2O_3$ 230.2
(III) (E)-2-chloro-N'-((furan-2-yl)methylene) benzohydrazide		$C_{12}H_9ClN_2O_2$ 248.7

given for the system to attain a steady state and the open circuit potential (OCP) was noted. The cathodic and anodic polarization curves were recorded at  $300 \text{ mV} \pm \text{OCP}$  by a sweep rate of  $2 \text{ mV s}^{-1}$ . The linear Tafel segments of the anodic and cathodic curves were extrapolated to the corrosion potential to obtain the corrosion current densities. The inhibition efficiency (% IE) values were calculated from  $i_{\text{corr}}$  as follows:<sup>28)</sup>

$$\% \text{ IE} = [1 - (i_{\text{corr}} / i_{\text{corr}}^0)] \times 100 \quad (2)$$

where  $i_{\text{corr}}^0$  and  $i_{\text{corr}}$  correspond to uninhibited and inhibited corrosion current densities, respectively.

### 2.5. AC impedance (EIS) studies

EIS experiments were carried out in the range of 100 kHz to 10 mHz at amplitude perturbation of 5 mV,<sup>29)</sup> using IM6e system (Zahner Elektrik, Germany) and personal computer. The impedance diagrams are given in Nyquist representation. Values of the charge transfer resistance ( $R_{\text{ct}}$ ) were obtained from these plots by determining the difference in the values of impedance at low and high frequencies. The double layer capacitance ( $C_{\text{dl}}$ ) and the frequency at which the imaginary component of impedance is maximal ( $-Z_{\text{max}}$ ) are found as follow:

$$C_{\text{dl}} = (1/2\pi f_{\text{max}} R_{\text{ct}}) \quad (3)$$

The inhibition efficiency and the surface coverage ( $\theta$ ) obtained from the impedance measurements are defined by the following equation:

$$\% \text{ IE} = \theta \times 100 = [1 \times (R_{\text{ct}}^0 / R_{\text{ct}})] \times 100 \quad (4)$$

where  $R_{\text{ct}}^0$  and  $R_{\text{ct}}$  are the charge transfer resistance in the absence and presence of inhibitor, respectively.

## 3. Results and Discussion

### 3.1. Weight loss method

Weight loss of carbon steel, in  $\text{mg cm}^{-2}$  of the surface area, was determined at various time intervals in the absence and presence of different concentrations ( $3 \times 10^{-5}$ - $15 \times 10^{-5}$  M) of the benzohydrazide derivatives (I-III). Fig. 1 shows the variation of the weight loss as a function of time, when the test pieces of carbon steel were allowed to react with 2 M HCl in presence of inhibitor (I). The curves obtained in the presence of

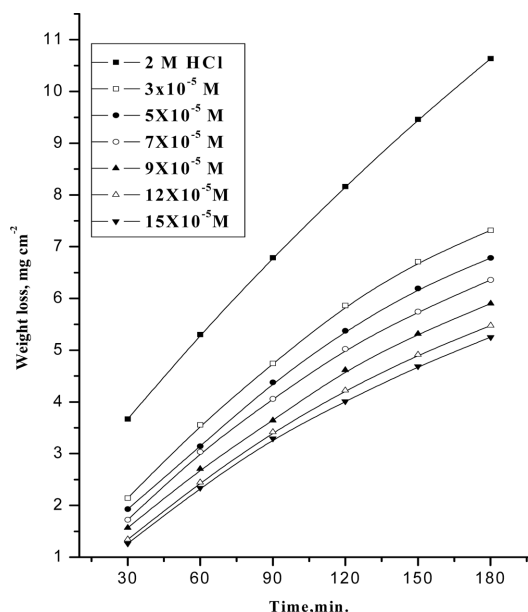


Fig. 1. Weight loss-time curves for carbon steel dissolution in 2 M HCl in the absence and presence of different concentrations of inhibitor (I) at 30°C.

different concentrations of inhibitors fall significantly below that of free acid. Similar behaviors were obtained for the other inhibitors (not shown). It is obvious that the weight loss varied linearly with immersion period in plain acid and inhibited acid, showing that the absence of insoluble product on carbon steel surface.<sup>30)</sup> Values of % IE are tabulated in Table 2. In all cases, the increase in the inhibitor concentration was accompanied by a decrease in the weight loss and an increase in % IE. These results lead to the conclusion that, these compounds under investigation are fairly efficient inhibitors for carbon steel dissolution in HCl solution. Careful inspection of these results showed that, at the same inhibitor concentration, the ranking of the inhibitors according to % IE is as follows: I > II > III.

#### 3.1.1. Synergistic effect

The effect of addition  $1 \times 10^{-2}$  M KI and KBr on the corrosion rate of carbon steel in the absence and presence of different concentrations of inhibitors (I-III) in 2 M HCl solutions was investigated using weight loss method. Results of % IE of KI obtained are summarized in Table 2. It was observed from these results that these additives improved the % IE significantly. The synergistic parameters were calculated using the relationship initially given by Aramaki and Hacker-

**Table 2.** Inhibition efficiency (% IE) of carbon steel at 90 min immersion in 2 M HCl in the presence of different concentrations of investigated additives at 30°C

Conc., M	% IE		
	(I)	(II)	(III)
$3 \times 10^{-5}$	69.5 (79.3)*	62.4 (71.3)	57.8 (66.1)
$5 \times 10^{-5}$	71.6 (82.4)	66.8 (74.5)	60.4 (96.1)
$7 \times 10^{-5}$	75.5 (84.8)	69.2 (77.3)	64.7 (72.3)
$9 \times 10^{-5}$	78.1 (87.2)	72.3 (80.3)	66.5 (75.4)
$12 \times 10^{-5}$	79.4 (90.0)	75.3 (83.4)	68.3 (79.6)
$15 \times 10^{-5}$	82.3 (92.1)	78.4 (86.5)	71.9 (81.5)

\*The values between brackets are the % IE in presence of  $1 \times 10^{-2}$  M KI.

**Table 3.** Synergism parameter ( $S_\theta$ ) for different concentrations of inhibitors for carbon steel dissolution in 2 M HCl with addition of  $1 \times 10^{-2}$  M KI at 30°C

Conc., M	Synergism parameter ( $S_\theta$ )		
	(I)	(II)	(III)
$3 \times 10^{-5}$	1.2	1.0	1.1
$5 \times 10^{-5}$	1.1	1.2	1.1
$7 \times 10^{-5}$	1.0	1.0	1.2
$9 \times 10^{-5}$	1.1	1.3	1.0
$12 \times 10^{-5}$	1.2	1.3	1.1
$15 \times 10^{-5}$	1.3	1.1	1.0

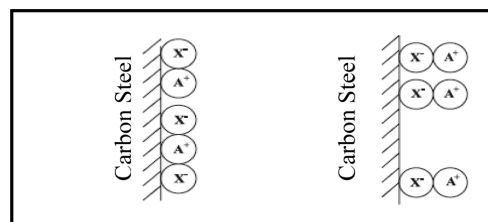
man and reported elsewhere:<sup>31)</sup>

$$S_\theta = \frac{1 - \theta_{1+2}}{1 - \theta_{1+2}} \quad (5)$$

where:  $\theta_{1+2} = (\theta_1 + \theta_2) - (\theta_1\theta_2)$

$\theta_1$  = the degree of surface coverage by the anions,  $\theta_2$  = the degree of surface coverage by the cations,  $\theta_{1+2}$  = measured surface coverage by both anions and cations.  $S_\theta$  approaches 1 when no interaction between the inhibitor molecules exists, while  $S_\theta > 1$  points to a synergistic effect. In the case of  $S_\theta < 1$ , the antagonistic interaction prevails.

Values of  $S_\theta$  are summarized in Table 3. These values are more than unity, suggesting that the phenomenon of synergism exists between the inhibitor molecules and these halides. Aramaki<sup>32,35)</sup> has proposed two kinds of joint adsorption (competitive and cooperative) to explain the synergistic action observed between an anion and a cation.<sup>36)</sup> For competitive adsorption, the anion and cation are adsorbed at different

**Fig. 2.** Schematic representations of (a) competitive and (b) cooperative adsorption of the anions (X) and cations (A<sup>+</sup>) on carbon steel surface in acid solutions.

sites on the electrode surface and for cooperative adsorption, the anion is chemisorbed on the surface and the cation is adsorbed on the layer of the anions. The two types of adsorption are represented schematically in Fig. 2 and can be characterized by a synergistic factor ( $S_\theta$ ) calculated as above.

The synergistic inhibitive effect brought about by combination of the inhibitors with KI and KBr for the corrosion of carbon steel in 2 M HCl can be explained as follows: The strong chemisorption of X ions (I or Br) on the metal surface is responsible for the synergistic effect of these ions, in attraction with protonated inhibitor.<sup>37)</sup> X ions are adsorbed on the anodic sites on the metal surface. Surface charge is changed to negative by the specific adsorption of these ions resulting in the joint adsorption of anions with the inhibitor cations. The inhibitors are believed to be adsorbable, not only on the cathodic sites by coulombic attraction using the charge of the protonated molecule, but also on the anodic sites by virtue of donation of the electron-pair on the nitrogen atom of the unprotonated molecule,<sup>34)</sup> therefore, interference adsorption can take place at the anodic sites.

### 3.1.2. Adsorption isotherm

Assuming the corrosion inhibition was caused by the adsorption of hydrazide derivatives, and the values of surface coverage for different concentrations of inhibitors in 2 M HCl were evaluated from weight loss. From the values of ( $\theta$ ), it can be seen that these values increased with increasing the concentration of benzohydrazide derivatives. Using these values of surface coverage, one can utilize different adsorption isotherms to deal with experimental data. The Temkin adsorption isotherm was applied to investigate the adsorption mechanism, by plotting ( $\theta$ ) vs. log C, and straight lines were obtained (Fig. 3). On the other hand, it was found that kinetic-thermodynamic model

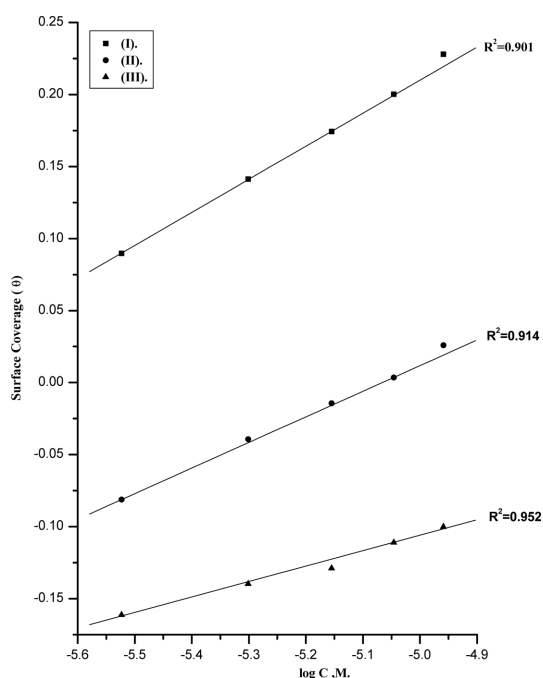


**Fig. 3.** Curve fitting of corrosion data for carbon steel in 2 M HCl in presence of different concentrations of organic additives to the Temkin adsorption isotherm at 30°C.

of El-Awady *et al.*<sup>38)</sup> can be applied (Fig. 4). This model has the formula:

$$\log (\theta / 1 - \theta) = \log K' - y \log C \quad (6)$$

The equilibrium constant of adsorption  $K = K^{(1/y)}$ , where  $1/y$  is the number of the surface active sites occupied by one compounds molecule and  $C$  is the bulk concentration of the inhibitor.

The thermodynamic parameters of the adsorption process obtained from these Figures are shown in Table 4. The values of  $\Delta G_{\text{ads}}^0$  are negative and increased as the % IE increased which indicate that

**Table 4.** Inhibitor equilibrium constant ( $K$ ), free energy of adsorption ( $\Delta G_{\text{ads}}^0$ ), number of active sites ( $1/y$ ) and the interaction parameter ( $a$ ) for inhibitors additives at 30°C

Inhibi- tors	Kinetic model			Temkin model		
	$1/y$	$K, \text{M}^{-1}$	$-\Delta G_{\text{ads}}^0, \text{kJ mol}^{-1}$	$a$	$K, \text{M}^{-1}$	$-\Delta G_{\text{ads}}^0, \text{kJ mol}^{-1}$
(I)	4.30	0.999	62.0	14.00	73.0	64.1
(II)	3.23	0.883	55.4	13.55	68.4	60.3
(III)	3.070	0.676	53.2	13.36	16.9	52.9

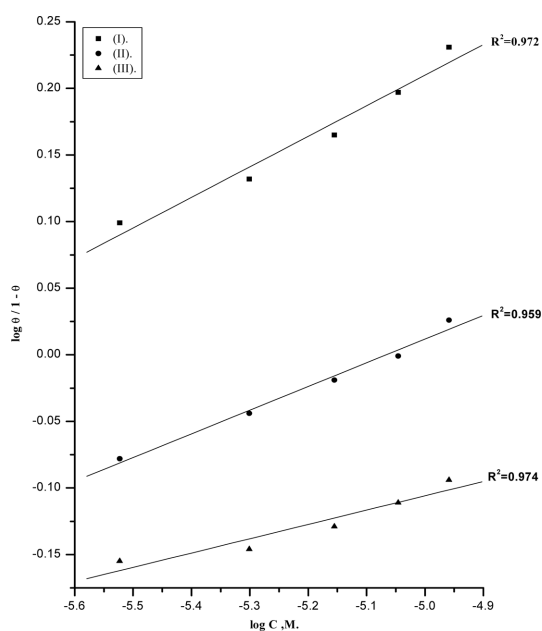


**Fig. 4.** Curve fitting of corrosion data for carbon steel in 2 M HCl in presence of different concentrations of organic additives to the kinetic model at 30°C.

these investigated compounds are strongly adsorbed on the C- steel surface and show the spontaneity of the adsorption process and stability of the adsorbed layer on the carbon steel surface. Generally, values of  $\Delta G_{\text{ads}}^0$  up to  $-20 \text{ kJ mol}^{-1}$  are consistent with the electrostatic interaction between the charged molecules and the charged metal (physical adsorption) while those more negative than  $-40 \text{ kJ mol}^{-1}$  involve sharing or transfer of electrons from the inhibitor molecules to the metal surface to form a coordinate type of bond (chemisorptions).<sup>39)</sup> The values of  $\Delta G_{\text{ads}}^0$  obtained were approximately equal to  $-53 \pm 1 \text{ kJ mol}^{-1}$ , indicating that the adsorption mechanism of the benzohydrazide derivatives on carbon steel in 2 M HCl solution involves both electrostatic adsorption and chemisorptions.<sup>40)</sup> The thermodynamic parameters point toward both physisorption (major contributor) and chemisorptions (minor contributor) of the inhibitors onto the metal surface. The values of  $K_{\text{ads}}$  follow the same trend in the sense that large values of  $K_{\text{ads}}$  imply better more efficient adsorption and hence better inhibition efficiency.<sup>41)</sup>

### 3.1.3. Effect of temperature

The activation energies ( $E_a^*$ ) for the corrosion of carbon steel in the absence and presence of different

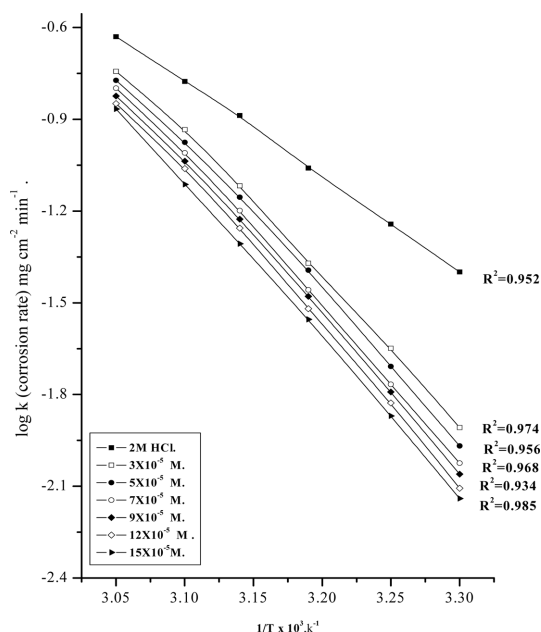


**Fig. 5.**  $\log k$  (corrosion rate) -  $1/T$  curves for carbon steel dissolution in 2 M HCl in the absence and presence of different concentrations of inhibitor (I).

concentrations of benzohydrazide derivatives were calculated using Arrhenius-type equation:<sup>42)</sup>

$$\log k = \log A - E_a^* / 2.303RT \quad (7)$$

where  $A$  is the pre-exponential factor,  $k$  is the rate constant,  $E_a^*$  is the apparent activation energy of the corrosion process,  $R$  is the universal gas constant and  $T$  is the absolute temperature. Arrhenius plots of  $\log k$  vs.  $1/T$  for carbon steel in 2 M HCl in the absence and presence of different concentration of inhibitors (I) are shown graphically in Fig. 5. The variation of  $\log k$  vs.  $1/T$  is a linear one and the values of  $E_a^*$  were calculated from the slope of these lines and given in Table 5. The increase in  $E_a^*$  with the addition of concentration of inhibitors (I-III) indicating that the energy barrier for the corrosion reaction increases. It is also indicated that the whole process is controlled by surface reaction, since the activation energy of the corrosion process is larger than  $20 \text{ kJ mol}^{-1}$ .<sup>42)</sup> Enthalpy and entropy of activation ( $\Delta H^*$ ,  $\Delta S^*$ ) for the corrosion of carbon steel in HCl were obtained by applying the transition state equation:<sup>42)</sup>

$$k = (RT / Nh) \exp(\Delta S^* / R) \exp(-\Delta H^* / RT) \quad (8)$$

**Table 5.** Activation parameters for the dissolution of carbon steel in the presence and absence of different concentrations of inhibitors in 2 M HCl at 30°C

Inhibitor	Conc., M.	Activation parameters		
		$E_a^*$ kJ mol <sup>-1</sup>	$\Delta H_a^*$ kJ mol <sup>-1</sup>	$-\Delta S_a^*$ J mol <sup>-1</sup> K <sup>-1</sup>
Free Acid (2 M HCl)	0	47.7	46.4	43.8
(I)	$3 \times 10^{-5}$	50.2	48.6	36.5
	$5 \times 10^{-5}$	52.8	51.2	32.4
	$7 \times 10^{-5}$	54.1	53.4	28.1
	$9 \times 10^{-5}$	56.5	54.8	22.9
	$12 \times 10^{-5}$	58.7	55.7	18.3
	$15 \times 10^{-5}$	61.9	57.8	15.9
(II)	$3 \times 10^{-5}$	49.1	47.2	38.4
	$5 \times 10^{-5}$	50.7	49.3	34.3
	$7 \times 10^{-5}$	52.1	50.8	30.7
	$9 \times 10^{-5}$	54.8	52.5	28.4
	$12 \times 10^{-5}$	55.4	53.8	24.1
	$15 \times 10^{-5}$	58.4	55.2	23.1
(III)	$3 \times 10^{-5}$	47.8	46.8	39.3
	$5 \times 10^{-5}$	48.4	48.6	34.9
	$7 \times 10^{-5}$	50.3	49.4	31.3
	$9 \times 10^{-5}$	51.7	50.8	29.7
	$12 \times 10^{-5}$	53.1	51.3	25.5
	$15 \times 10^{-5}$	54.7	53.2	24.5

where  $h$  is Planck's constant,  $N$  is Avogadro's number. A plot of  $\log k/T$  vs  $1/T$  also gave straight lines as shown in Fig. 6 for carbon steel dissolution in 2 M HCl in the absence and presence of different concentration of inhibitor (I). The slopes of these lines equal  $-\Delta H^* / 2.303R$  and the intercept equal  $\log RT/Nh + (\Delta S^* / 2.303R)$  from which the value of  $\Delta H^*$  and  $\Delta S^*$  were calculated and tabulated in Table 5. From these results, it is clear that the presence of the tested compounds increased the activation energy values and consequently decreased the corrosion rate of the carbon steel. These results indicate that these tested compounds acted as inhibitors through increasing activation energy of carbon steel dissolution by making a barrier to mass and charge transfer by their adsorption on carbon steel surface. Positive sign of the enthalpies reflects the endothermic nature of the steel dissolution process.

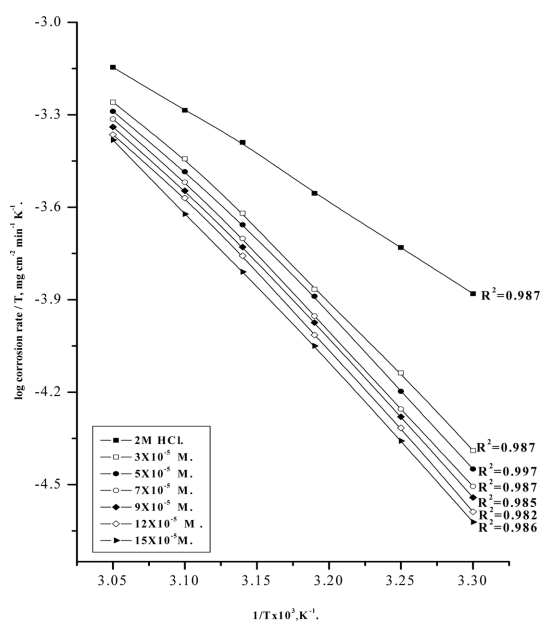


**Fig. 6.**  $\log(\text{corrosion rate}/T) - (1/T)$  curves for carbon steel dissolution in 2 M HCl in the absence and presence of different concentrations of inhibitor (I).

All values of  $E_a^*$  are larger than the analogous values of  $\Delta H^*$  indicating that the corrosion process must involve a gaseous reaction, simply the hydrogen evolution reaction, associated with a decrease in the total reaction volume.<sup>44)</sup>

The values of  $\Delta S^*$  in absence and presence of the tested compounds are large and negative; this indicates that the activated complex in the rate-determining step represents an association rather than dissociation step, meaning that a decrease in disordering takes place on going from reactants to the activated complex.<sup>45,46)</sup>

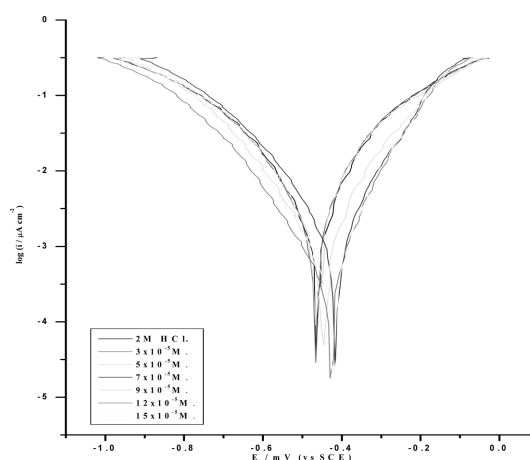


**Fig. 7.** Potentiodynamic polarization curves for carbon steel in 2 M HCl in the absence and presence of different concentrations of inhibitor (I) at 30°C.

### 3.2. Potentiodynamic polarization measurements

The cathodic and anodic polarization curves for carbon steel in 2 M HCl solution in absence and presence of various concentrations of the inhibitors (I) at 30°C are shown in Fig. 7. Similar curves were obtained for other inhibitors (not shown). The various electrochemical parameters calculated from Tafel plots are given in Table 6. The lower corrosion current density ( $i_{\text{corr}}$ ) values in presence of the inhibitors without causing significant changes in corrosion potential ( $E_{\text{corr}}$ ) suggest that the investigated compounds are mixed type inhibitors and are adsorbed on the surface thereby blocking the corrosion reaction.<sup>47)</sup>

The results also show that the slopes of the anodic and the cathodic Tafel slopes ( $\beta_a$  and  $\beta_c$ ) were slightly changed on increasing the concentration of the tested compounds. This indicates that there is no change in

**Table 6.** The effect of concentration of compound (I) on the free corrosion potential ( $E_{\text{corr}}$ ), corrosion current density ( $i_{\text{corr}}$ ), Tafel slopes ( $\beta_a$  &  $\beta_c$ ), inhibition efficiency (% IE), degree of surface coverage ( $\theta$ ) and corrosion rate (CR) for the corrosion of carbon steel in 2 M HCl at 30°C

Conc., M	$-E_{\text{corr}}$ , mV	$i_{\text{corr}}$ , $\mu\text{A cm}^{-2}$	$\beta_c$ , mV dec <sup>-1</sup>	$\beta_a$ , mV dec <sup>-1</sup>	% IE	CR, mm y <sup>-1</sup>
0.0	467	82.0	311	283	0.000	95.2
$3 \times 10^{-5}$	467	31.8	207	175	0.612	37.0
$5 \times 10^{-5}$	460	31.7	217	180	0.613	36.8
$7 \times 10^{-5}$	412	12.7	183	124	0.845	14.8
$9 \times 10^{-5}$	452	4.7	173	139	0.943	5.4
$12 \times 10^{-5}$	449	2.0	144	119	0.976	2.3
$15 \times 10^{-5}$	428	1.3	147	106	0.984	1.5

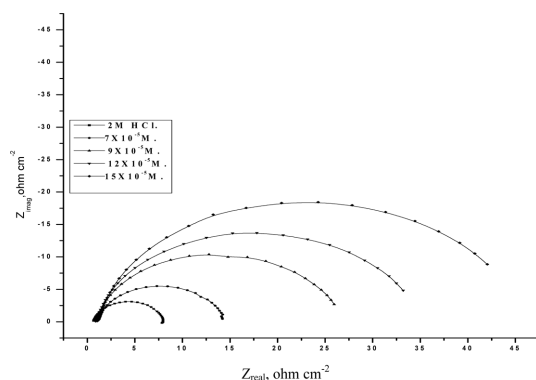


**Fig. 8.** The Nyquist plots for carbon steel in 2 M HCl solution in the absence and presence of different concentrations of inhibitor (I) at 30°C.

the mechanism of inhibition in presence and absence of inhibitors. The values of  $\beta_c$  are slightly higher than the values of  $\beta_a$  suggesting a cathodic action of the inhibitor. The higher values of Tafel slope can be attributed to surface kinetic process rather the diffusion-controlled process.<sup>48)</sup>

### 3.3. Electrochemical impedance spectroscopy measurements

The inhibition efficiencies of investigated compounds on carbon steel surface were examined by electrochemical impedance spectroscopy. The impedance spectra (Nyquist plot) of carbon steel in 2 M HCl solution in the absence and presence of different concentrations of inhibitor (I) were recorded in Fig. 8. Similar curves were obtained for other inhibitors (not shown). The impedance diagrams display one single capacitive loop represented by slightly depressed semi-circle for all studied compounds. This capacitive loop indicates that the corrosion of carbon steel in 2 M HCl solution is mainly controlled by charge transfer process and formation of a protective layer on the metal surface. Deviation from the ideal semi-circle are generally attributed to the frequency dispersion as well as inhomogeneities, roughness of metal surface and mass transport process.<sup>49-51)</sup> The diameter of the capacitive loop increases as the concentration of inhibitor molecules on the surface.<sup>52)</sup> On the other hand, the similar nature of the impedance diagrams obtained in the absence and presence of investigated compounds reveal that the addition of the inhibitors does not change the mechanism for the dissolution of carbon steel in HCl.<sup>53-55)</sup>

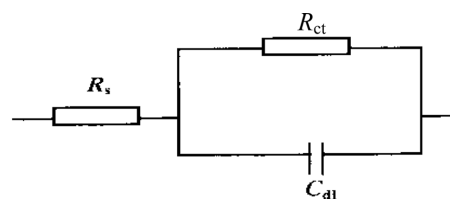


**Fig. 9.** The equivalent circuit model used to fit the experimental results.

All experimental spectra were fitted with an appropriate equivalent circuit to find the parameters, which describe and being consistent with the experimental data. Fig. 9 depicts the proposed equivalent circuit, which consists of  $R_s$ ,  $R_{ct}$  and  $C_{dl}$  which refer to solution resistance, charge transfer resistance and capacitance of double layer, respectively.

EIS parameters and % IE were calculated and tabulated in Table 7. In order to correlate impedance and polarization methods,  $i_{corr}$  values were obtained from polarization curves and Nyquist plots in the absence and presence of different concentrations of inhibitors (I-III).

It was observed from the obtained EIS data that  $R_{ct}$  increases and  $C_{dl}$  decreases with the increasing of inhibitor concentration. The increase in  $R_{ct}$  values, and consequently of inhibition efficiency, may be due to the gradual replacement of water molecules by the adsorption of the inhibitor molecules on the metal surface to form an adherent film on the metal surface. This suggests that the film formation on the metal surface will decrease the double layer thickness.<sup>56)</sup> Also, this decrease of  $C_{dl}$  at the metal/solution interface with increasing the inhibitor concentration can result from a decrease in local dielectric constant which indicates that the inhibitors were adsorbed on the surface at both anodic and cathodic sites.<sup>57)</sup>

**Table 7.** Electrochemical kinetic parameter obtained by EIS technique for the corrosion of carbon steel 2 M HCl at different concentration of compound (I) at 30°C

Conc., M	$C_{dl}$ , $\mu\text{F cm}^{-2}$	$R_{ct}$ , $\Omega \text{ cm}^2$	$\theta$	% IE
0	119.31	6.894	0.000	0.0
$7 \times 10^{-5}$	108.8	13.97	0.507	50.7
$9 \times 10^{-5}$	104.64	24.62	0.720	72.0
$12 \times 10^{-5}$	103.7	34.52	0.800	80.0
$15 \times 10^{-5}$	96.8	41.03	0.832	83.2



The impedance data confirm the inhibition behavior of the inhibitors obtained with other techniques. From the data of Table 7, it can be seen that the  $i_{\text{corr}}$  values decrease significantly in the presence of these additives and the % IE is greatly improved. The order of reduction in  $i_{\text{corr}}$  exactly correlates with that obtained from potentiodynamic polarization studies. Moreover, the decrease in the values of  $i_{\text{corr}}$  follows the same order as that obtained for the values of  $C_{\text{dl}}$ . It can be concluded that the inhibition efficiency found from weight loss, polarization curves, electrochemical impedance spectroscopy measurements are in good agreement.

#### 4. Mechanism of Corrosion Inhibition

The inhibition efficiency of the studied three derivatives namely: (I) 2-Methyl-benzoic acid (5-formyl-3H-furan-2-ylidene)-hydrazide, (II) 2-Hydroxy-benzoic acid (5-formyl-3H-furan-2-ylidene)-hydrazide and (III) 2-Chloro-benzoic acid (5-formyl-3H-furan-2-ylidene)-hydrazide, for carbon steel in 2 M HCl is in the order: (I) > (II) > (III). The extent of inhibition depends on the active centers and the electron density (donating or with drawing) of the substituent groups.

In acid medium benzohydrazide derivatives get protonated at nitrogen atoms of the hydrazide group, which results in the formation of positively charged inhibitor species, thus adsorption of the inhibitor on the carbon steel surface may occur through the following ways: i) The electronic configuration of Fe is  $[\text{Ar}] 3d^6 4s^2$ . Thus, vacant 3d orbitals of iron can bond with inhibitor due to interaction of electron rich  $\pi$ -electron clouds of aromatic rings as well as unshared electron pairs on nitrogen or oxygen atoms of the inhibitor. ii) The protonated inhibitor could be attached to the steel surface which is negatively charged in hydrochloric acid medium due to the specifically adsorbed  $\text{Cl}^-$  ions on the metal surface. Thus adsorption can occur via electrostatic interaction between positively charged inhibitor molecules and negatively charged metal surface.<sup>58,59)</sup>

The decrease in the inhibition efficiency with increase in temperature suggests that adsorption of the inhibitor occurs mainly by physisorption involving electrostatic interaction of the protonated inhibitors and the negatively charged metal surface.

Compound (I) exhibits excellent inhibition power due to the presence of two nitrogen, two oxygen atoms and  $\text{CH}_3$  group (highly electron releasing group)

which enhance the delocalized  $\pi$ -electrons on the active centers of the compound. Compound (II) comes after compound (I) in inhibition efficiency in spite of it has two nitrogen, two oxygen atoms and one OH group. Unfortunately, this compound may form complex compound with  $\text{Fe}^{2+}$  and screen the sharing effect of one oxygen atom and one nitrogen atom. Compound (III) has the lowest inhibition efficiency. This is due to it has two nitrogen, two oxygen atoms and Cl-atom. The presence of Cl-atom (which is electron withdrawing group) lowers the electron density on the molecule and hence, lowers its inhibition efficiency, so it becomes the least effective one.

#### 5. Conclusions

In this paper, electrochemical methods were used to study the ability of investigated derivatives to inhibit the corrosion of carbon steel in 2 M HCl solution. The principal conclusions are:

- 1) The inhibition efficiency of investigated derivatives increases by increasing the inhibitor concentration, but it decreases with increase in temperature.
- 2) The polarization curves indicated that the investigated derivatives inhibit cathodic hydrogen evolution and anodic metal dissolution reactions. These derivatives act as mixed-type inhibitors.
- 3) Ac impedance plots of investigated derivatives indicated that polarization resistance increases with increase in inhibitor concentration.
- 4) The adsorption of these inhibitors on the metal surface from 2 M HCl solution obeys Temkin adsorption isotherm and kinetic model. The negative sign of  $\Delta G_{\text{ads}}^{\circ}$  indicates that the Adsorption process is spontaneous.
- 5) The increase in activation energy after the addition of inhibitors to the 2 M HCl solution indicates that the adsorption is more physical than chemical.
- 6) On addition of halide anions to 2 M HCl containing inhibitors, a synergistic or cooperative effect occurred thus increasing the inhibiting effect of carbon steel corrosion.

#### References

1. H. Keles and M. Keles, *Mater. Chem. Phys.*, **112**, 173 (2008).
2. A. Chetouani, B. Hammouti, T. Benhadda, and M. Daoudi, *Appl. Surf. Sci.*, **249**, 375 (2005).
3. S. Sankarap, F. Apavinasam, M. Pushpanaden, and F.

- Ahmed, *Corros. Sci.*, **32**, 193 (1991).
4. A. B. Tadros and Y. Abdel-Naby, *J. Electroanal. Chem.*, **224**, 433 (1988).
  5. N. C. Subramanyam, B. S. Sheshardi, and S. A. Mayanna, *Corros. Sci.*, **34**, 563 (1993).
  6. B. Babu, Ramesh and K. Thangavel, *Anti-Corros. Meth. Mater.*, **52**, 219 (2005).
  7. A. S. Fouda, H. A. Mostafa, F. El-Taib Haekel, and G. Y. Elewady, *Corros. Sci.*, **47**, 1988 (2005).
  8. R. Yurchenko, L. Pogrebova, T. Pilipenko, and T. Shubina, *Russian J. Appl. Chem.*, **79**, 1100 (2006).
  9. S. A. Hossain and A. L. Almarshad, *Corros. Eng. Sci. Technol.*, **41**, 77 (2006).
  10. S. M. Abd El-Wahaab, G. K. Gomma, and H. Y. El-Barradie, *J. Chemical Technol. Biotechnol.* **36**, 435 (2007).
  11. S. Muralidharan and S. V. K. Iyer, *Anti-Corros. Meth. Mater.* **44**, 100 (1997).
  12. M. A. Quraishi, M. A. W. Khan, and M. Ajmal, *Anti-Corros. Meth. Mater.* **43**, 5 (1996).
  13. Bentiss, M. Traisnel, and M. Lagrenee, *J. Appl. Electrochem.*, **31**, 41 (2001).
  14. M. Sahin and S. Bilgic, *Anti-Corros. Meth. Mater.*, **50**, 34 (2003).
  15. M. Lebrini, F. Bentiss, H. Vezin, and M. Lagrenée, *Corros. Sci.*, **48**, 1279 (2006).
  16. M. Lebrini, M. Lagrenee, H. Vezin, M. Traisnel, and F. Bentiss, *Corros. Sci.*, **49**, 2254 (2007).
  17. K. M. Ibrahim, T. H. Rakha, A. M. Abdallah and M. M. Hassanain, *Ind. J. Chem.*, **32A**, 361 (1993).
  18. T. Tsuru, S. Haruyama, and G. Boshoku, *J. Japan Soc. Corrs. Eng.*, **27**, 573 (1978).
  19. L. Larabi, Y. Harek, M. Traisnel, and A. Mansri, *J. Appl. Electrochem.*, **34**, 833 (2004).
  20. K. Aramaki, M. Hagiwara, and H. Nishihara, *Corros. Sci.*, **27**, 487 (1987).
  21. K. Aramaki, *Corros. Sci.*, **44**, 871 (2002).
  22. G. K. Gomma, *Mater. Chem. Phys.*, **55**, 241 (1998).
  23. Y. Harek and L. Larabi, *Kem. Ind.*, **53**(2), 55 (2004).
  24. E. E. Oguzie, *Mater. Chem. Phys.*, **87**, 212 (2004).
  25. E. Kalman, I. Lukovits, and G. Palinkas, *ACH Models Chem.*, **132**(4), 527 (1995).
  26. D. Q. Zhang, L. X. Gao, and G. D. Zhou, *J. Appl. Electrochem.*, **33**, 361 (2003).
  27. A. S. Fouda, M. F. El-Sherbiny, and M. M. Motawea, *Desalination and Water Treatment*, **30**, 207 (2011).
  28. S. A. Abd El-Maksoud and A. S. Fouda, *Mater. Chem. Phys.*, **93**, 84 (2005).
  29. J. Aljourani, K. Raieisi, and M. A. Colozar, *Corros. Sci.*, **51**, 1836 (2009).
  30. A. K. Singh and M. A. Quraishi, *Corros. Sci.*, **51**, 2752 (2009).
  31. M. Bouklah, B. Hammouti, A. Aouniti, M. Benkaddour, and A. Bouyanzer, *Appl. Surf. Sci.*, **252**, 6236 (2006).
  32. K. Aramaki, M. Hagiwara, and H. Nishihara, *J. Electrochem. Soc.*, **134**, 1896 (1987).
  33. K. Aramaki and H. Nishihara, *J. Electrochem. Soc.*, **134**, 1059 (1987).
  34. K. Aramaki, M. Hagiwara, and H. Nishihara, *Corros. Sci.*, **27**, 487 (1987).
  35. K. Aramaki, *Corros. Sci.*, **44**, 871 (2002).
  36. N. Ochoa, F. Moran, and N. Pebere, *J. Appl. Electrochem.*, **34**, 487 (2004).
  37. L. Larabi and Y. Harek, *Port. Electrochim. Acta*, **22**, 227 (2004).
  38. Y. A. El-Awady, A. K. Mohamed, A. A. El-Shafei, and M. Abo El-Wafa, *Bull. Electrochem.*, **17**(17), 145 (2001).
  39. F. Bensajjay, S. Alehyen, M. El Achouri, and S. Kertit, *Anti-Corros. Meth. Mater.*, **50**, 402 (2003).
  40. S. Z. Duan and Y. L. Tao, *Interface Chem. Higher Education Press, Beijing*, 124 (1990).
  41. S. S. Abd El-Rehim, S. A. M. Refaey, F. Taha, M. B. Saleh, and R. A. Ahmed, *J. Appl. Electrochem.* **31**, 429 (2001).
  42. I. N. Putilova, S. A. Balezin, and V. P. Barannik, *Metallic Corrosion Inhibitors, Pergamon Press, New York*, p. 31, (1960).
  43. K. K. Al-Neami, A. K. Mohamed, I. M. Kenawy, and A. S. Fouda, *Monatsh Chem.*, **126**, 369 (1995).
  44. E. A. Noor, *Int. J. Electrochem. Sci.*, **2**, 996 (2007).
  45. J. Marsh, *Advanced Organic Chemistry, 3<sup>rd</sup> ed, Wiley Eastern, New Delhi*, (1988).
  46. S. Martinez, *Appl. Surf. Sci.*, **199**, 83 (2002).
  47. R. T. Vashi and V. A. Champaneri, *Indian J. Chem. Technol.*, **180**, (1997).
  48. A. K. Mohamed, H. A. Mostafa, G. Y. El-Awady, and A. S. Fouda, *Port. Electrochim. Acta*, **18**, 99 (2000).
  49. R. Solmaz, E. Altunbas, and G. Kardas, *Mater. Chem. Phys.*, **125**, 796 (2011).
  50. A. Chetouani, A. Aouniti, B. Hammouti, N. Benchat, T. Benhadda, and S. Kertit, *Corros. Sci.*, **45**, 1675 (2003).
  51. M. Behpour, S. M. Ghoreishi, N. Soltani, and M. Salavati-Niasari, *Corros. Sci.*, **51**, 1073 (2009).
  52. R. Solmaz, *Corros. Sci.*, **52**, 3321 (2010).
  53. S. S. Abd El Rehim, H. H. Hassan, and M. A. Amin, *Mater. Chem. Phys.*, **78**, 337 (2002).
  54. Q. Zhang and Y. Hua, *Mater. Chem. Phys.*, **119**, 57 (2010).
  55. K. F. Khaled, *Corros. Sci.*, **52**, 2905 (2010).
  56. A. S. Fouda, A. M. El-Defrawy, and M. W. El-Sherbeni, *J. Electrochem. Sci. Technol.*, **4**(2), 1 (2013). <http://dx.doi.org/10.5229/JECST.2013.4.2.1>
  57. F. Mansfeld, *Electrochim. Acta*, **35**, 1533 (1990).
  58. I. B. Obot, N. O. Obi-Egbedi, and S. A. Umoren, *Corros. Sci.*, **51**, 1868 (2009).
  59. W. H. Li, Q. He, S. T. Zhang, C. L. Pei, and B. R. Hou, *J. Appl. Electrochem.*, **38**, 289 (2008).